

Application of Molecular Modelling and EPR Spectroscopy to Lipid Membranes – a Combined Approach

Andrea Catte and Vasily S. Oganessian*

School of Chemistry, University of East Anglia, Norwich, NR4 7TJ, United Kingdom

*E-mail: v.oganesyan@uea.ac.uk

Received 15 January 2016

Abstract. Knowledge of molecular interactions, thermodynamics, temperature and system composition effects are crucial for understanding the role that different lipids play in vital life processes in biological membranes. This knowledge is also important for understanding the impact that electromagnetic fields have on the order and mobility of molecules in lipid bilayers.

The last decade has seen radical improvement in the molecular modelling of complex molecular and bio-molecular systems including lipid bilayers using Molecular Dynamics (MD) simulation techniques. MD simulations are now much faster and more accurate allowing researchers to predict complex molecular phenomena using actual structures. In this paper we present our recent results on the application of large scale MD simulations to phospholipid bilayers under different composition and conditions. Examples include: both all-atom and coarse-grain large scale MD simulations of binary and ternary compositions of lipid bilayers, modelling of the penetration of gas molecules (O_2) in lipid bilayers, the effects of antimicrobial peptides on biological membranes, separation of lipid microdomains as a model for the study of lipid rafts. We also report MD simulations on lipid bilayers doped with structurally different nitroxide spin probes that are employed in experimental variable temperature EPR spectroscopy. Finally, our recent preliminary results of all-atom MD modelling of the lipid bilayers subjected to microwave electric fields are also presented and discussed.

Keywords: Molecular dynamics (MD) simulations; lipid bilayers; antimicrobial peptides; EPR spectroscopy; spin probes; microwave electric fields.

Phospholipid bilayers with different lipid compositions have been extensively investigated and employed as models of biological membranes over the past decades[1]. Dipalmitoylphosphatidylcholine (DPPC), the major component of the lung surfactant, which is a mixture of lipids and proteins lining the surface of the alveoli in the lungs and it is essential for breathing, has been widely studied with experimental and computational techniques. Pure DPPC lipids exhibit a gel or solid ordered (S_o) phase to liquid crystalline (L_α) phase transition at 41°C , which is also known as the chain melting temperature. The L_α phase of DPPC is also usually named as the liquid disordered (L_d) phase. The presence of cholesterol (CHOL) induces an ordering of the acyl chains of DPPC and other saturated lipids leading to the formation of a liquid ordered (L_o) phase. This structural change is attributed to the well-known condensing effect of CHOL[2]. The coexistence of L_d and L_o phases has also been observed in giant unilamellar vesicles containing CHOL and two types of lipids. The phase diagrams of DPPC:CHOL binary and ternary systems with temperature are characterised by a variety of coexisting phases.

MD simulations with doped spin probes for EPR spectral predictions and analysis

Of the biophysical techniques now being brought to bear on studies of membranes Electron Paramagnetic Resonance (EPR) of nitroxide spin probes was the first to provide information about mobility and ordering in lipid membranes and lipid bilayer systems. EPR is a ‘fast’ spectroscopic technique that can resolve molecular re-orientational dynamics of the

introduced spin probe on sub-nanosecond timescales. Spin probes, specially designed chemical agents that carry a stable unpaired electron, can be introduced within complex partially ordered molecular systems in order to report on the order and dynamics of surrounding molecules. EPR spin probes containing nitroxide groups at different positions in the fatty acid chain, such as 1-palmitoyl-2-stearoyl-(n-doxy)-sn-glycero-3-phosphocholines (n-PC spin probes), and in the CHOL head group, such as 3 β -doxyl-5 α -cholestane (CSL), have been used to study the structure of lipids [3, 4] and their interaction with membrane proteins [5]. Structurally variable spin probes can probe different depths/parts of the bilayer and also be attached to embedded peptides and proteins.

EPR spectra of biological membranes can be predicted directly from the results of MD using our original MD-EPR simulation methodology [6, 7] that has been successfully applied previously to liquid crystals and proteins [8-10]. The advantage of such an approach is twofold. Firstly, it allows detailed analysis and unambiguous conclusions about molecular motions and organisation in lipid bilayers. Secondly, our MD-EPR methodology serves as a test bed for advanced computational models for lipid bilayers simulations. We apply this methodology to address the key problems of understanding molecular interactions and system composition effects on the formation and dynamics of lipid domains, the organisation and dynamics of lipids around trans-membrane proteins, and the role of cholesterol as a lipid bilayer stabiliser. Here we report the MD simulation part of our work that includes the development of an accurate set of force field parameters for different spin probes and large scale modelling of a mixed systems at fully atomistic level. The example of all atom structure of a DPPC lipid bilayer doped with CSL spin probes equilibrated after 100 ns at 298 K together with the structure of the lipid and different spin probes is shown in Fig. 1.

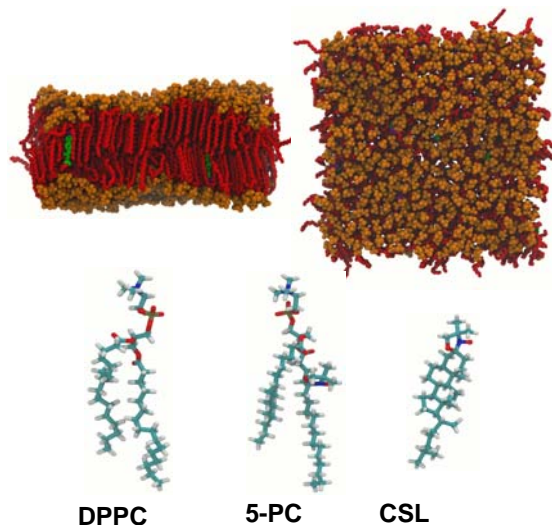


Fig. 1. Snapshot of a typical simulation with the doped spin probes. Top and side views of the 100 ns structure of a DPPC lipid bilayer with 598 DPPC and 2 CSL spin probe molecules simulated at 298 K and 1 atm. DPPC polar headgroups and hydrophobic acyl chains are in orange space filling and red licorice representations, respectively. CSL spin probes cholesterol and nitroxide moieties are in green and purple licorice representations, respectively. The licorice representations of DPPC and spin probes are also shown.

AA MD simulations were performed using Gromacs version 4.5.5 [11]. A refined version of the CHARMM36 force field in Gromacs, which is known as the Stockholm lipids (Slipids) force field, was used for lipids [12]. Force field parameters for spin probes were calculated using Gaussian version 09 [13] and Amber version 12 [14]. Non-bonded van der Waals and electrostatics interactions were truncated using a cut-off distance of 12 Å. The PME treatment of long range electrostatic interactions was employed. Temperature and pressure for all simulated DPPC lipid bilayers were stabilized at 298 K and 1 atm using a Nosé-Hoover thermostat [15] and a Parrinello-Rahman barostat [16], respectively. Coordinate trajectories

were updated every 20 ps for all AA MD simulations. Each DPPC lipid bilayer was solvated with 30 water molecules per lipid and ionized with a proper amount of Na⁺ and Cl⁻ ions to reach a physiological ionic strength of 150 mM. Total number of atoms, including water and ions, reached values of approximately 132,000 atoms. The resulting long MD trajectories are used for prediction of motional EPR spectra at different temperatures.

Modelling of the penetration of O₂ molecules across DPPC lipid bilayer.

The 35 ns AA MD simulation of a DPPC lipid bilayer containing 1200 lipids interacting with 100 O₂ molecules at 298 K and 1 atm shows the penetration of O₂ molecules in the lipid bilayer as described in Fig. 2. The concentration of O₂ molecules, which was estimated from the oxygen partial density profile, reaches a maximum in the bilayer centre. This result is in agreement with previous experimental and computational results reported by Al-Abdul-Wahid et al. in 2006 [17].

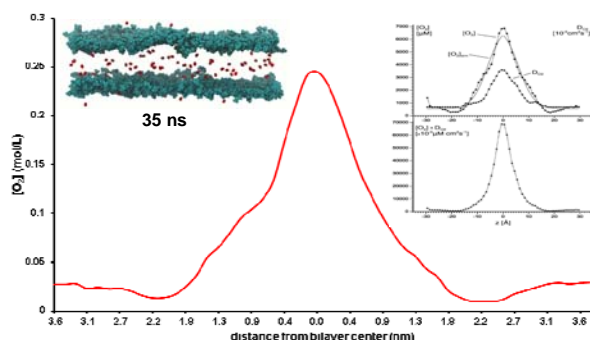


Fig. 2. Oxygen concentration as a function of immersion depth estimated from O₂ partial density profile of a 35 ns AA MD simulation of a DPPC lipid bilayer with 1200 lipids and 100 O₂ molecules simulated at 298 K and 1 atm. DPPC polar headgroups and oxygen molecules are in cyan and red space filling representations, respectively. The inset shows similar experimental and computational plots reported by Al-Abdul-Wahid et al. in 2006[17].

Interestingly, the presence of O₂ molecules induces an ordering of DPPC sn-1 and sn-2 acyl chains as observed in the plots of the order parameter profiles on the left panel of Fig. 3. Moreover, the diffusion coefficients of O₂ molecules estimated from the mean squared displacements of the gas molecules over the last 41.5 ns of a 101.5 ns AA MD simulation show that the lateral diffusion is larger than the translational diffusion as reported in the right panel of Fig. 3.

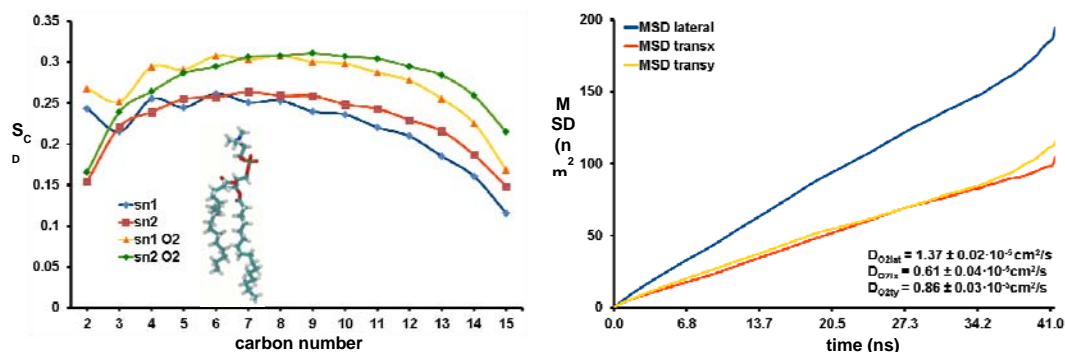


Fig. 3. DPPC sn-1 and sn-2 acyl chains order parameter profiles in the absence and in the presence of O₂ molecules estimated from AA MD simulations at 298 K and 1 atm (left). Mean squared displacement (MSD) employed to estimate lateral and translational diffusion coefficients of O₂ molecules using the last 41.5 ns of a 101.5 ns AA MD simulations (right).

Modelling the effects of antimicrobial peptides on biological membranes.

The interaction of palmitoylcholine (POPC), which is the main lipid component of egg PC, in the presence of the recently discovered antimicrobial peptide chrysopsin-3 (chrys-3) [18] has also been investigated performing CG MD simulations of a POPC lipid bilayer with transmembrane peptides using an approach similar to the one reported by Thøgersen et al in 2008 [19]. CG MD simulations were performed using the MARTINI force field for lipids [20] and proteins [22].

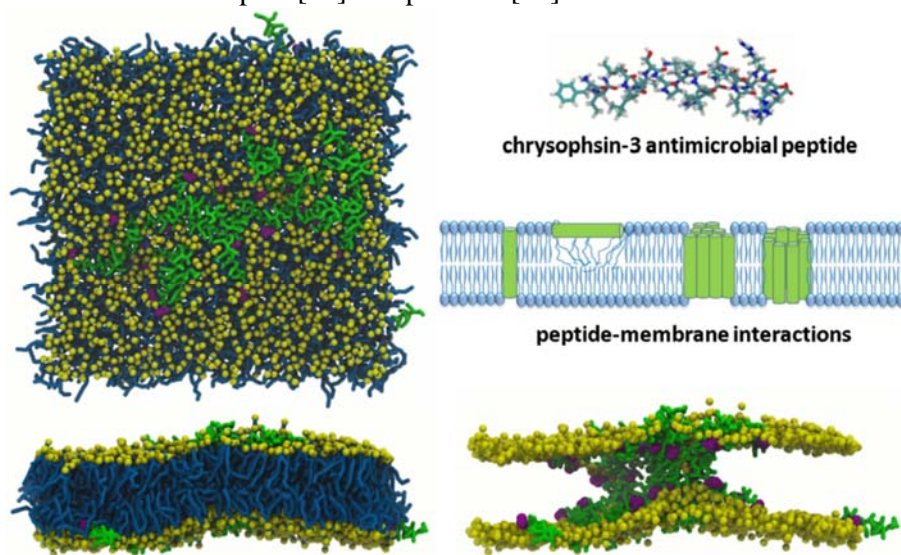


Fig. 4. Top and side views of a CG POPC lipid bilayer containing 1058 lipids with 50 chrysopsin-3 antimicrobial peptides CG MD simulated for 16 μ s at 310 K and 1 atm. POPC polar headgroups and hydrophobic acyl chains are shown in yellow space filling and skyblue/licorice representations, respectively. Chrysopsin-3 peptides are shown in green licorice representation with purple space filling phenylalanine residues. The licorice representation of the AA structure of the 20 amino acid antimicrobial peptide is also shown together with a cartoon depicting the different types of peptide-membrane interactions proposed by Wang et al. in 2015[21].

The standard cut-offs of the MARTINI force field were used for non-bonded interactions: the Lennard-Jones potential was shifted to zero between 0.9 and 1.2 nm, and the Coulomb potential was shifted to zero between 0 and 1.2 nm with a relative dielectric constant of 15. The time step was 20 fs, and the neighbour list was updated every 10 steps [23]. Lipids and water were coupled separately to a target temperature using the velocity rescaling thermostat [24] with a time constant of 1 ps. A target surface tension was maintained using the surface tension coupling scheme and the Berendsen barostat [25] with a time constant of 4 ps and a compressibility of $5 \times 10^{-5} \text{ bar}^{-1}$ in the lateral direction; the compressibility in the normal direction was set to zero to prevent box contraction. Each POPC lipid bilayer was solvated with 10 CG waters (corresponding to 40 real water molecules) per lipid and ionized with a proper amount of Na^+ and Cl^- .

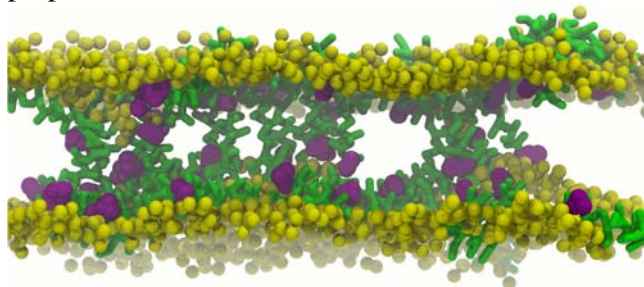


Fig. 5. Side view of the 16 μ s CG POPC lipid bilayer containing 1058 lipids with 50 chrysopsin-3 antimicrobial peptides simulated at 310 K and 1 atm. POPC hydrophobic acyl chains are not shown for clarity. The colour code is the same of Fig. 4. The formation of two distorted toroidal pores and a transmembrane aggregate is observed in agreement with Wang et al. 2015 experimental results [21].

ions to reach a physiological ionic strength of 150 mM. CG MD simulations with regular and polarizable CG water yield similar results. After 16 μ s of CG MD simulation the peptides aggregate on the surface and in the transmembrane region forming two distorted toroidal pores and an aggregate as shown in Fig 4. All four types of peptide-membrane interactions, as reported experimentally by Wang et al. in 2015 and shown in their cartoon of Fig. 4 [21], are observed during the CG MD simulation as shown in Fig. 5.

Ternary lipid mixtures (DPPC:DOPC:CHOL) CG MD simulations – separation of lipid microdomains.

CG and AA MD simulations of ternary lipid systems containing CHOL:DPPC:DOPC mixtures with different molar ratios have also been performed in order to sample the different phase behaviour using as a reference the experimental work of Veatch et al. 2007 [26] as shown in Fig. 7. Initially, we performed 40 μ s CG MD simulations of the different ternary lipid systems with a random distribution of lipids in order to observe the formation of L_o and L_d domains. CG MD simulations were performed using the MARTINI force field for lipids [20]. DOPC force field parameters were the same used by Risselada et al. in 2008[27]. CG MD simulations with regular and polarizable CG water yield similar results. Then, AA structures were reconstructed from a selection of 40 μ s CG structures as shown in Fig. 7. The fine graining of CG structures was performed using previously reported approaches[28]. Each fine grained structure was also subjected to several steps of energy minimizations in order to remove steric clashes. These fine grained structures can be used as starting models for the insertion of EPR spin probes or for the study of the interaction of antimicrobial peptides with ternary lipid systems (work in progress).

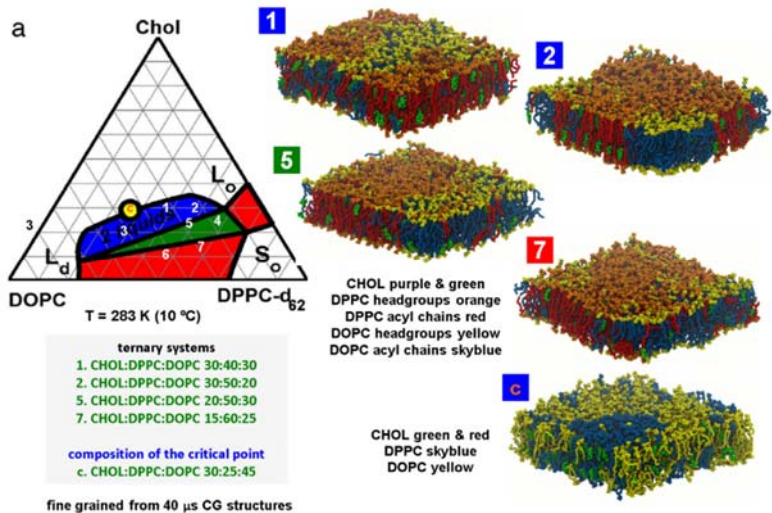


Fig. 7. Ternary phases diagram of CHOL:DPPC:DOPC from Veatch et al. 2007 experimental work[26]. AA ternary systems fine grained from 40 μ s CG structures to be simulated in the presence of EPR spin probes.

systems can also be useful to study the formation of lipid rafts as previously reported by Risselada et al. in 2008 and as shown in Fig. 8 [27]. CHOL molecules interact more with saturated lipids (DPPC) forming L_o domains, while the unsaturated lipids (DOPC) show less interactions with CHOL and

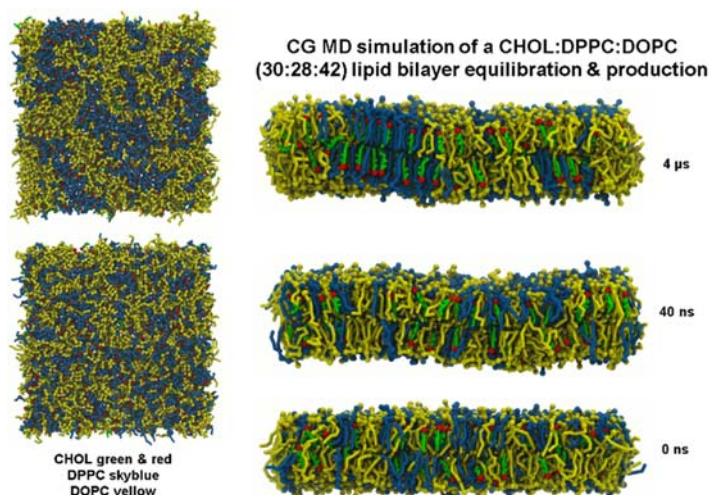


Fig. 8. CG MD simulation of a CHOL:DPPC:DOPC lipid bilayer can be used to study the formation of lipid rafts.

CG MD simulations of ternary lipid form L_d domains. CG MD simulations allow to sample longer timescales. This is achieved because of the unified atom models used to represent molecules and the possibility to use longer timesteps for the integration of forces. A comparison between AA and CG structures of lipids employed in ternary lipid systems is shown in Fig. 9. The resolution of atomistic details is still kept and can be restored by fine graining the CG MD simulated structures as shown in Fig. 10[28].

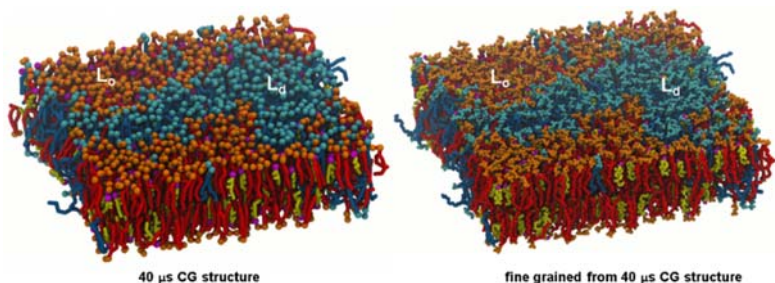


Fig. 9. Fine graining of the 40 μs structure of CHOL:DPPC:DOPC (30:40:30) ternary lipid system.

All-atom MD simulation of lipid bilayers in the presence of microwave electric field; Electroporation.

The non-ionising effects of radiation on biological membranes, in particular electroporation, can also be studied through AA MD simulations of lipid bilayers subjected to external oscillating electric fields[29-31].

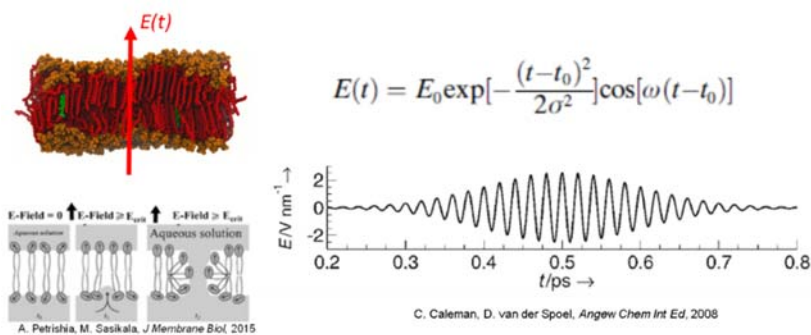


Fig. 11. Oscillating electric field applied to a DPPC lipid bilayer.

More recently, we have also performed AA MD simulations of DPPC and DOPC lipid bilayers in the presence of an oscillating electric field as shown in Fig. 12. In both AA MD simulations we observe the formation of pores applying an oscillating electric field of 0.5 V/nm with the microwave frequency of 2.5 GHz. Electroporation is observed at 3.72 ns and 6.24 ns, respectively. Preliminary results indicate that the effect of microwave field is primarily on the water molecules and that the electroporation occurs as the result of the changes in the interaction of water with phospholipid molecules.

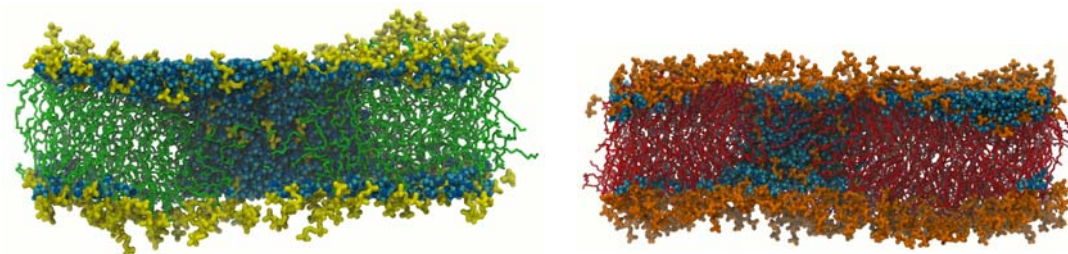


Fig. 12. Left: Formation of a pore after 3.72 ns in a DPPC lipid bilayer containing 600 lipids (30 waters/lipid) simulated at 323 K and 1atm applying an oscillating electric field of 0.5 V/nm with a frequency of 2.5 GHz. Right: Formation of a pore after 6.24 ns in a DOPC lipid bilayer containing 256 lipids (45 waters/lipid) simulated at 300 K and 1atm applying an oscillating electric field of 0.5 V/nm with a frequency of 2.5 GHz.

Acknowledgment.

VSO acknowledges the financial support of this project by EPSRC (EP/L001322/1).

References

- [1]. G. van Meer, D. R. Voelker, G. W. Feigenson, *Nat. Rev. Mol. Cell. Biol.* 9, 112-124 (2008).
- [2]. G.W. Feigenson, J. T. Buboltz, *Biophys. J.* 80, 2775-2788 (2001).
- [3]. W.K. Subczynski, J. Widomska, J. B. Feix, *Free Radical Biology & Medicine* 46, 707-718 (2009).
- [4]. F.T. Presti, S. I. Chan, *Biochemistry* 21, 3821-3830 (1982).
- [5]. D. Marsh, *Eur Biophys J* 39, 513-525 (2010).
- [6]. V.S. Oganessian, *SPR: Electron Paramagnetic Resonance*, (Eds: B.C. Gilbert, V. Chechik, D.M. Murphy), Royal Society of Chemistry, London, 24, 32-61, (2015).
- [7]. V.S. Oganessian, *Phys. Chem. Chem. Phys.* 13, 4724-4737 (2011).
- [8]. F. Chami, M. R. Wilson, V. S. Oganessian, *Soft Matter* 8, 6823-6833 (2012).
- [9]. H. Gopee, A. N. Cammidge, V. S. Oganessian, *Angew. Chem. Int. Ed.* 52, 8917-8920 (2013).
- [10]. E. Kuprusevicius, G. White, V. S. Oganessian, *Faraday Discuss.* 148, 283-298 (2011).
- [11]. S. Pronk, S. Páll, R. Schulz, P. Larsson, P. Bjelkmar, R. Apostolov, M. R. Shirts, J. C. Smith, P. M. Kasson, D. van der Spoel, B. Hess, E. Lindahl, *Bioinformatics* 29, 845-854 (2013).
- [12]. J.P.M. Jämbeck, A. P. Lyubartsev, *J. Phys. Chem. B* 116, 3164-3179 (2012).
- [13]. M.J. Frisch, G. W. Trucks, H. B. Schlegel Wallingford CT (2009).
- [14]. D.A. Case, T. A. Darden, T. E. Cheatham, et al., (2012).
- [15]. S. Nosé, *J. Chem. Phys.* 81, 511-519 (1984).
- [16]. M. Parrinello, A. J. Rahman, *J. Appl. Phys.* 52, 7182-7190 (1981).
- [17]. M.S. Al-Abdul-Wahid, C.-H. Yu et al., *Biochemistry* 45, 10719-10728 (2006).
- [18]. N. Iijima, N. Tanimoto, Y. Emoto, Y. Morita, K. Uematsu, T. Murakami, T. Nakai, *Eur. J. Biochem.* 270, 675-686 (2003).
- [19]. L. Thøgersen, B. Schjøtt, T. Vosegaard, N. C. Nielsen, E. Tajkhorshid, *Biophys. J.* 95, 4337-4347 (2008).
- [20]. S.J. Marrink, H. J. Risselada, S. Yefimov, D. P. Tieleman, A. H. de Vries, *J. Phys. Chem. B* 111, 7812-7824 (2007).
- [21]. K.F. Wang, R. Nagarajan, T. A. Camesano, *Biophys. Chem.* 196, 53-67 (2015).

- [22]. L. Monticelli, S. K. Kandasamy, X. Periole, R. G. Larson, D. P. Tieleman, S. J. Marrink, *J. Chem. Theor. Comput.* 4, 819-834 (2008).
- [23]. S. Baoukina, E. Mendez-Villuendas, W. F. D. Bennett, D. P. Tieleman, *Faraday Discuss.* 161, 63-75 (2013).
- [24]. G. Bussi, D. Donadio, M. Parrinello, *J. Chem. Phys.* 126, 014101 (2007).
- [25]. H.J.C. Berendsen, J. P. M. Postma, W. F. van Gunsteren, A. DiNola, J. R. Haak, *J. Chem. Phys.* 81, 3684-3690 (1984).
- [26]. S.L. Veatch, O. Soubias, S. L. Keller, K. Gawrisch, *Proc. Natl. Acad. Sci. USA* 104, 17650 -17655 (2007).
- [27]. H.J. Risselada, S. J. Marrink, *Proc. Natl. Acad. Sci. USA* 105, 17367-17372 (2008).
- [28]. T.A. Wassenaar, K. Pluhackova, R. Böckmann, S. J. Marrink, D. P. Tieleman, *J. Comput. Theor. Chem.* 10, 676-690 (2014).
- [29]. A. Petrishia, M. Sasikala, *J. Membrane Biol.* 248, 1015-1020 (2015).
- [30]. C. Caleman, D. van der Spoel, *Angew. Chem. Int. Ed.* 47, 1417-1420 (2008).
- [31]. D.P. Tieleman, H. Leontiadou, A. E. Mark, S. J. Marrink, *J. Am. Chem. Soc.* 125 6382-6383 (2003).